Supporting Information

Asymmetric Restriction of Intramolecular Rotation in Chiral Solvents

Young-Jae Jin,[†] Hyojin Kim,[†,‡] Jong Jin Kim,[§] Nam Ho Heo,[§] Jong Won Shin,[*,||] Masahiro Teraguchi,[⊥] Takashi Kaneko,[⊥] Toshiki Aoki[*,⊥] and Giseop Kwak[*,†]

[†]School of Applied Chemical Engineering, Major in Polymer Science and Engineering, Kyungpook National University 1370 Sankyuk-dong, Buk-ku, Daegu 702–701, Korea

*Email: gkwak@knu.ac.kr

[‡]Daegu Technopark Nano Convergence Practical Application Center, 891–5 Daecheon-dong, Dalseo-ku, Daegu 704–801, Korea

[§]School of Applied Chemical Engineering, Major in Applied Chemistry, Kyungpook National University, 1370 Sankyuk-dong, Buk-ku, Daegu 702–701, Korea

[||]Beamline Department Pohang Accelerator Laboratory, POSTECH, 80 Jigokro-127-beongil, Nam-gu Pohang, Gyeongbuk, Korea

*Email: jwshin@postech.ac.kr

[⊥]Department of Chemistry and Chemical Engineering, Graduate School of Science and Technology, and Center for Transdisciplinary Research, Niigata University, Ikarashi 2-8050, Nishi-ku, Niigata 950-2181, Japan

*Email: toshaoki@eng.niigata-u.ac.jp

Experimental section

Materials: TPE (purity >98.0, GC), TPB (purity >99.0, GC), PPCPD (purity >98.0, GC), TPCPD (purity >98.0, GC), and HPB were purchased from TCI in Japan (Tokyo Chemical Industry Co. Ltd.). The (+)-limonene (>99.0% ee grade: $[\alpha]^{20}_{D}$ +115.5±1°, c = 10% in ethanol), (–)-limonene (>99.0% ee grade: $[\alpha]^{20}_{D}$ –94±4°, c = 10% in ethanol), (+)-pinene (>99.0% ee grade: $[\alpha]^{21}_{D}$ +50.7°, neat) and (–)-pinene (99.0% ee grade: $[\alpha]^{20}_{D}$ –50.0°, neat) were purchased from Sigma-Aldrich.

Recrystallization of MRs in chiral solvent: All MR samples were heated in the appropriate chiral solvent solution (1-5 wt%) at 130 °C for 30 min and then cooled down to room temperature slowly to produce crystals. The excess solvent was removed by blotting using paper (Yuhan Kimberly, Ltd.) and the crystal was then rinsed with alcohol before drying in an oven at 60 °C for 3 days.

Measurements: The CD/UV-vis spectra of MR solutions were measured on a JASCO J-815 spectrometer, while the DR-CD/DR-UV-vis spectra of the MR crystals were measured with an integrating sphere compartment. The FL quantum yields of the solutions were recorded using a JASCO FP-6500 spectrofluorometer according to literature method using a quinine sulfate solution as a reference material.[S1] The absolute FL quantum yields of MR crystals were determined with an integrating sphere and a quantum efficiency calculation program. FL photographs were taken using a digital camera (Cannon PowerShot A2000 IS) under UV lamp of > 365 nm. Polarized microscope images were recorded using a Nikon Eclipse E600 microscope equipped with a digital camera (Nikon DS-Fi1) and a high-pressure mercury lamp (OSRAM, HBO103W/2). DSC was performed using a SETARAM DSC141-evo at a heating and cooling rate of 10 °C min^{-1} under

N2 flow. Single crystal X-ray diffraction data for the compounds were collected at 100(2) K using synchrotron radiation on an ADSC Quantum-210 detector at 2D SMC with a silicon (111) double crystal monochromator (DCM) at the Pohang Accelerator Laboratory, Korea (λ = 0.61000 – 0.63000 Å). The PAL BL2D-SMDC software[S2] was used for data collection (detector distance; 63 mm, omega scan; $\Delta\omega$ = 1º, exposure time; 1 sec per frame). Cell refinement, reduction and absorption correction were performed using HKL3000sm (Ver. 703r) program.[S3] The crystal structures were solved by direct methods[S4] with SHELXS-2014, and refined by full–matrix least–squares calculation on F^2 with SHELXL-2014 computer program.[S5] The all non–hydrogen atoms were refined with anisotropic displacement parameters and all hydrogen atoms were assigned geometrically using a riding model and constrained to ride on their parent atoms. The crystallographic data and the result of refinements are summarized in Table S3.

S1) Jin, Y.-J.; Bae, J.-E.; Cho, K.-S.; Lee, W.-E.; Hwang, D.-Y.; Kwak, G. *Adv. Funct. Mater.* **2014**, *24*, 1928-1937.

S2) Shin, J. W.; Eom, K.; Moon, D. *J. Synchrotron Rad*. **2016**, *23*, 369-373.

S3) Otwinowski Z.; Minor, W. *Methods in Enzymology*, Academic Press: New York, 1997, vol. 276, part A, p. 307.

S4) Sheldrick, G. M. *Acta Crystallogr., Sect. A.* **1990**, *46*, 467-473.

S5) Sheldrick, G. M. *Acta Crystallogr. Sect. C*. **2015**, *71*, 3-8.

Figure S1. a) Rotational DR-CD, DR-UV, and b) LD spectra of TPE crystals obtained from chiral limonenes.

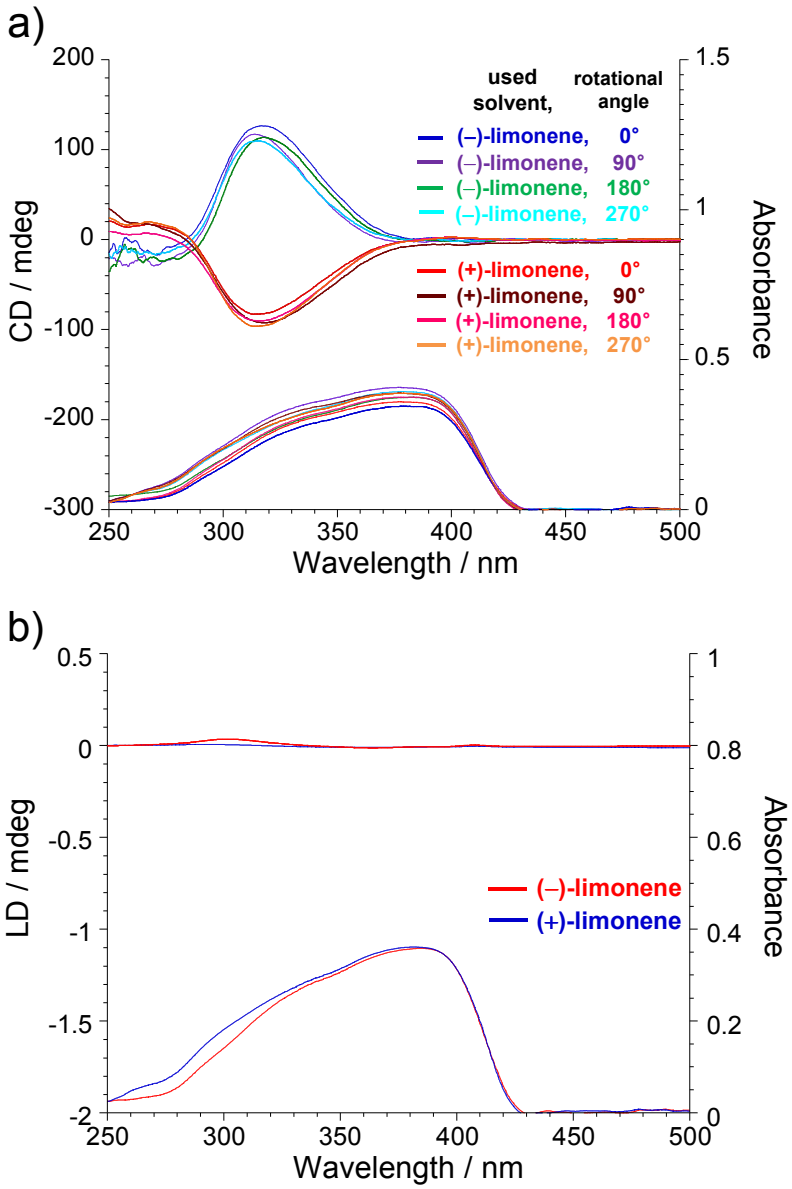

Figure S2. a) DR-CD and DR-UV spectra of TPE crystals obtained from chiral α-pinenes and CD and UV spectra of TPE in chiral α-pinene solutions, and b) rotational DR-CD and DR-UV spectra of the TPE crystal.

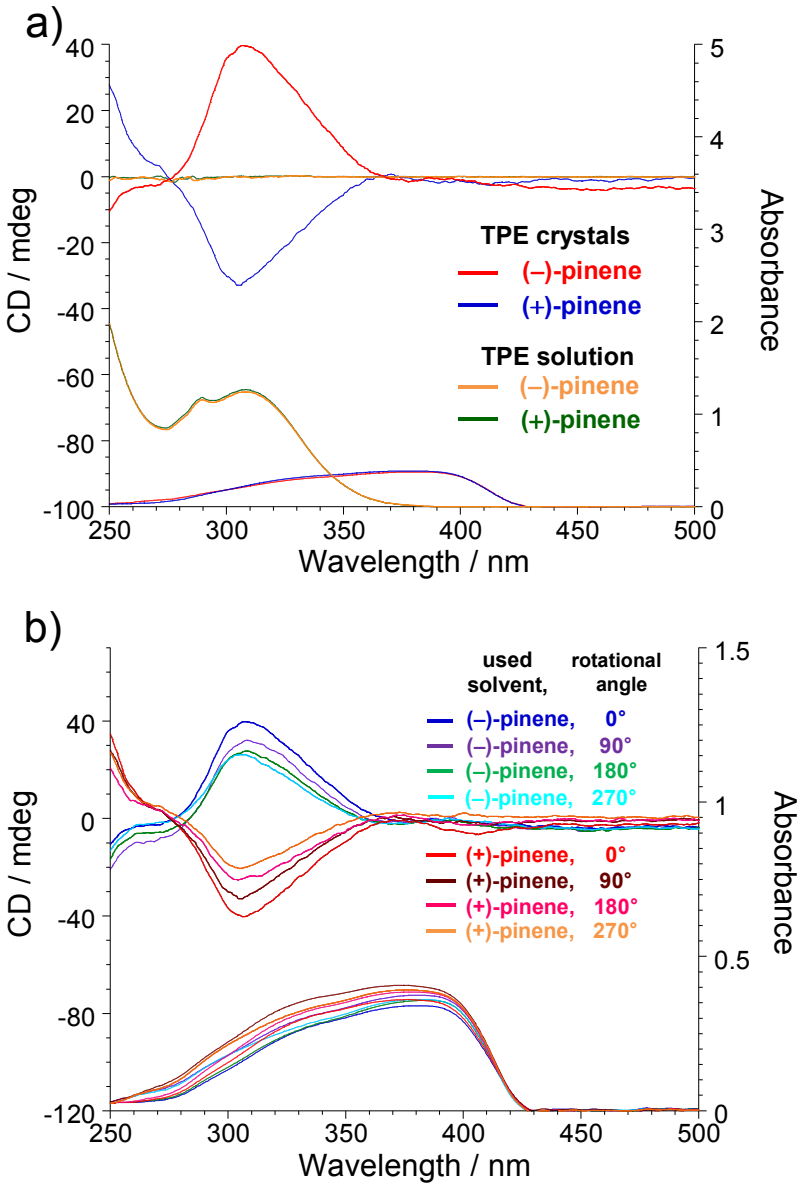

Figure S3. DR-CD and DR-UV spectra of the chiral crystals of a) TPB, b) PPCPD, and c) TPCPD recrystallized from chiral limonenes.

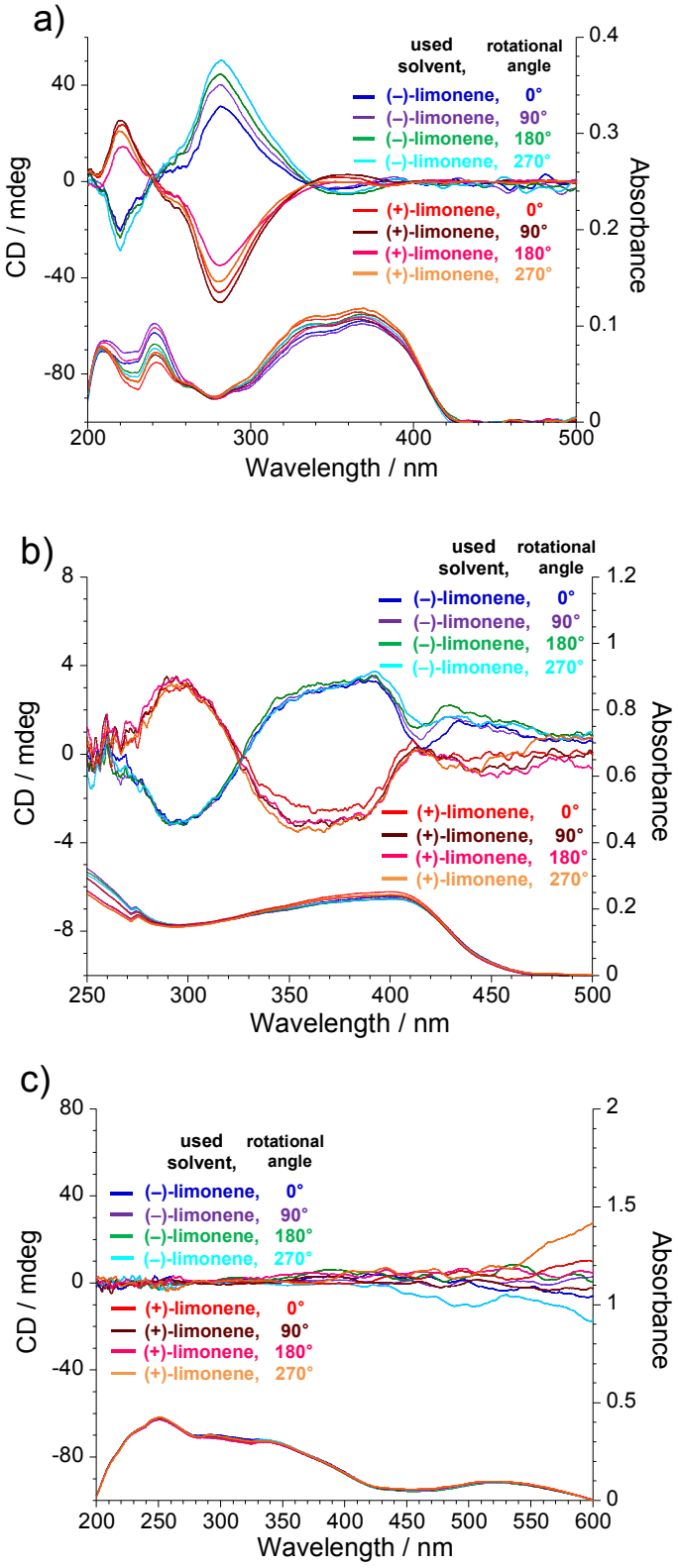

Figure S4. CD and UV absorption spectra of a) TPB, b) PPCPD, c) TPCPD in (–)-limonene (red line) and (+)-limonene (blue line) solutions.

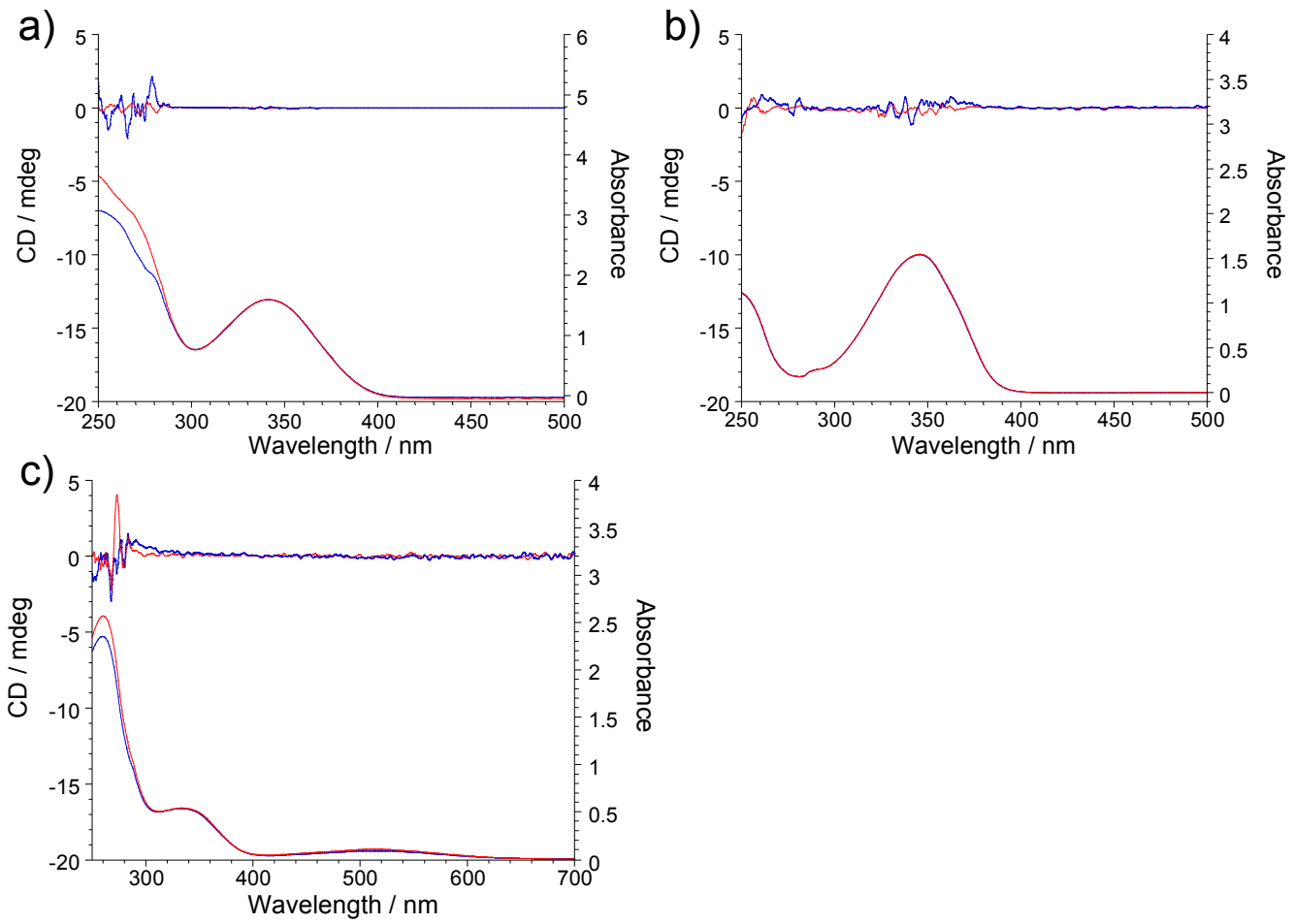

Table S1. Essential crystallographic data for TPE crystals recrystallized from chiral limonenes and α-pinenes

	Crystal from (–)-limonene	Crystal from (+)-limonene	Crystal from (–)-α-pinene	Crystal from (+)-α-pinene
Space group	$P2_1$	$P2_1$	$P2_1$	$P2_1$
a (Å)	9.790(2)	9.786(2)	9.790(2)	9.786(2)
b (Å)	9.1950(18)	9.2050(18)	9.1960(18)	9.2060(18)
c (Å)	10.781(2)	10.773(2)	10. 782(2)	10.773(2)
β (°)	107.98(3)	107. 92(3)	107.94(3)	107. 92(3)
V (Å^3)	923.1(3)	923.4(4)	923.3(4)	923.5(4)
Z	2	2	2	2
torsion angle (°) (C20-C7-C6-C5)	–44.98(19)	45.5(2)	-45.60(19)	46.02(16)
torsion angle (°) (C7-C20-C19-C18)	137.86(13)	–137.72(14)	137.62(14)	-137.39(12)
torsion angle (°) (C7-C20-C21-C26)	–47.65(18)	47.39(19)	-56.20(17)	56.32(15)
torsion angle (°) (C20-C7-C8-C13)	123.90(14)	–124.16(15)	132.84(14)	-132.99(12)

Figure S5. Crystal structures of TPE obtained from chiral α-pinenes: a) ORTEP images with thermal ellipsoids plotted at the 50% probability level, and b) schematic illustration.

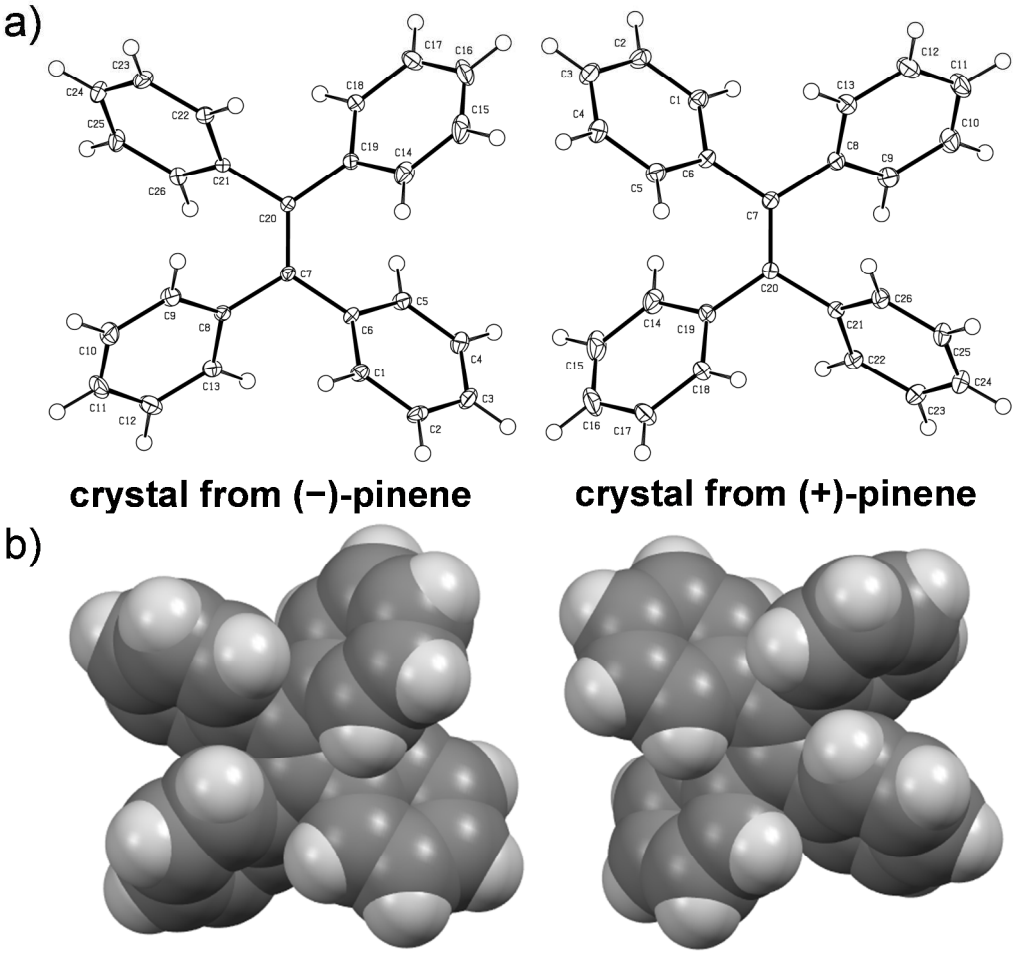

Figure S6. The enantiomorphs of chiral TPE crystals as observed by optical microscopy.

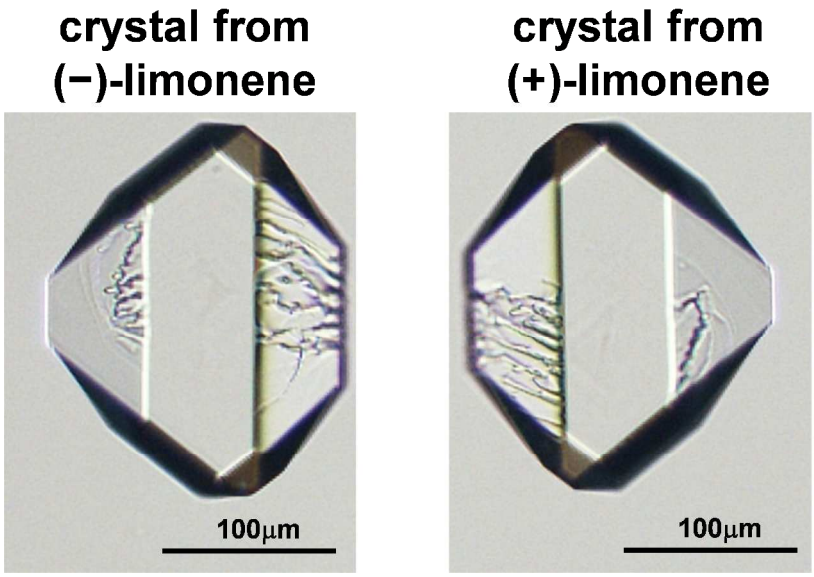

Figure S7. DSC thermograms of TPE crystals during heating (heating rate = 10 °C min^{-1}).

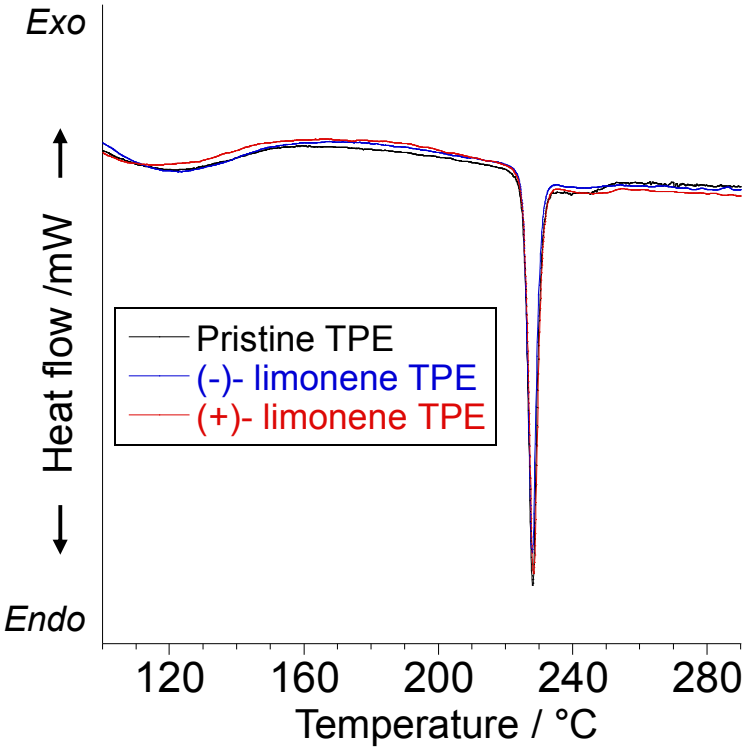

Table S2. FL emission properties of MRs in THF solutions and in the crystalline state

chiral solvent, MR	FL properties			
	in THF solution		in crystal state	
	$\lambda_{max,\,FL}$ (nm)	Φ_{FL} (%)[a)]	$\lambda_{max,\,FL}$ (nm)	Φ_{FL} (%)[b)]
(–)-limonene, TPE	474	0.018	447	23.4
(+)-limonene, TPE	472	0.016	448	23.6
(–)-pinene, TPE	471	0.017	447	24.1
(+)-pinene, TPE	472	0.019	448	24.3
(–)-limonene, TPB	442	0.22	437	91.2
(+)-limonene, TPB	446	0.26	437	92.7
(–)-limonene, PPCPD	445	0.26	471	22.0
(+)-limonene, PPCPD	444	0.23	472	21.8

[a)]Determined as relative fluorescence quantum yield using the reference point method. $\Phi_s = \Phi_r(A_rF_s/A_sF_r)(\eta_s^2/\eta_r^2)$, where Φ is the quantum yield, F is the measured integrated fluorescence emission intensity, A is the absorbance at λ_{max} and η is the refractive index of the solvent. The subscript 'r' refers to the reference with a known quantum yield and 's' denotes the sample. More detailed information was described in the experimental section. [b)]Determined as absolute fluorescence quantum yield with an integrating sphere and quantum efficiency calculation program at an excitation wavelength of 360 nm.

Figure S8. Crystal structures of TPCPD obtained from chiral limonenes: a) ORTEP images with thermal ellipsoids plotted at the 50% probability level. All hydrogen atoms have been omitted for clarity. b) Schematic illustration.

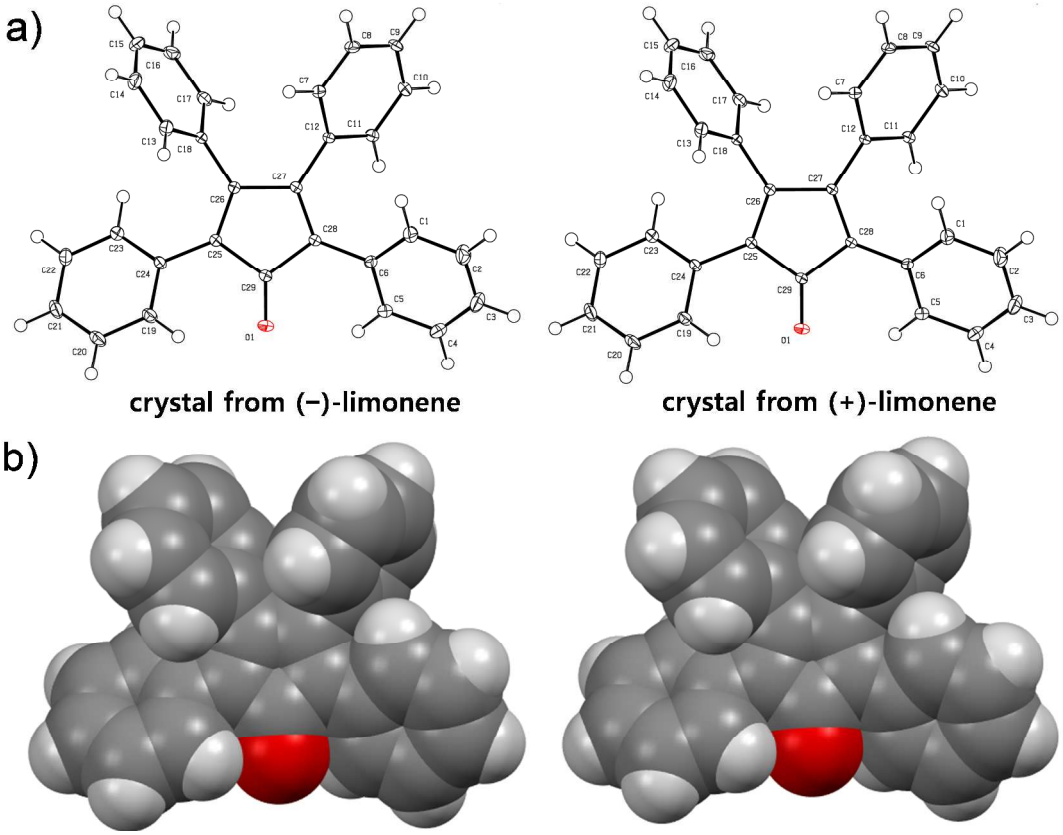

Table S3. Crystallographic data and structure refinement for MR crystals

data	crystal					
	(−)-limonene TPE	(+)-limonene TPE	(−)-pinene TPE	(+)-pinene TPE	(−)-limonene TPCPD	(+)- limonene TPCPD
Empirical formula	$C_{26}H_{20}$	$C_{26}H_{20}$	$C_{26}H_{20}$	$C_{26}H_{20}$	$C_{29}H_{20}O$	$C_{29}H_{20}O$
Formula weight	332.42	332.42	332.42	332.42	384.45	384.45
Crystal system	Monoclinic	Monoclinic	Monoclinic	Monoclinic	Monoclinic	Monoclinic
Space group	$P2_1$	$P2_1$	$P2_1$	$P2_1$	$C2/c$	$C2/c$
Color	colorless	colorless	colorless	colorless	red-violet	red-violet
Crystal size, mm^3	0.200 × 0.200 × 0.150	0.120 × 0.100 × 0.100	0.160 × 0.140 × 0.100	0.120 × 0.100 × 0.080	0.070 × 0.060 × 0.040	0.080 × 0.050 × 0.020
a, Å	9.790(2)	9.786(2)	9.790(2)	9.786(2)	26.139(5)	26.167(5)
b, Å	9.1950(18)	9.2050(18)	9.1960(18)	9.2060(18)	8.2000(16)	8.1980(16)
c, Å	10.781(2)	10.773(2)	10.782(2)	10.773(2)	21.507(4)	21.500(4)
β, deg	107.98(3)	107.92(3)	107.93(3)	107.92(3)	119.81(3)	119.84(3)
V, $Å^3$	923.1(3)	923.4(4)	923.3(3)	923.5(4)	3999.9(17)	4000.5(17)
Z	2	2	2	2	8	8
d_{calc}, g cm^{-3}	1.196	1.196	1.196	1.195	1.277	1.277
λ, Å	0.61000	0.61000	0.61000	0.61000	0.63000	0.61000
T, K	100(2)	100(2)	100(2)	100(2)	100(2)	100(2)
μ, mm^{-1}	0.051	0.051	0.054	0.054	0.060	0.057
F(000)	352	352	352	352	1616	1616
Reflections collected	9202	9380	9225	14616	20146	19843
Independent reflections	5002	5085	5001	8011	5570	5549
Reflections with $I>2\sigma(I)$	4959	4995	4957	7673	4637	4858
Goodness-of-fit on F^2	1.058	1.041	1.057	1.051	1.034	1.057
Final R indices $[I>2\sigma(I)]$[a)]	R_1 = 0.0340	R_1 = 0.0346	R_1 = 0.0339	R_1 = 0.0399	R_1 = 0.0436	R_1 =0.0423
	wR_2 = 0.0909	wR_2 = 0.0923	wR_2 = 0.0904	wR_2 = 0.1087	wR_2 = 0.1155	wR_2 =0.1173
Final R indices [all data][a)]	R_1 = 0.0349	R_1 = 0.0353	R_1 = 0.0348	R_1 = 0.0419	R_1 = 0.0537	R_1 =0.0480
	wR_2 = 0.0911	wR_2 = 0.0927	wR_2 = 0.0906	wR_2 = 0.1099	wR_2 = 0.1226	wR_2 =0.1216

[a)] $R_1 = \Sigma||F_o| - |F_c||/\Sigma|F_o|$, $wR_2 = [\Sigma w(F_o^2 - F_c^2)^2/\Sigma w(F_o^2)^2]^{1/2}$.